Impact of Pad Layouts and Solder Volume on Self-Alignment of Micro Solar Cells

Elisa Kaiser
Fraunhofer Institute for Solar Energy Systems ISE
Freiburg, Germany
elisa.kaiser@ise.fraunhofer.de

Maike Wiesenfarth
Fraunhofer Institute for Solar Energy Systems ISE
Freiburg, Germany
maike.wiesenfarth@ise.fraunhofer.de

Victor Vareilles
Université Grenoble Alpes, CEA LITEN
Campus INES,
Le Bourget du Lac, France
victor.vareilles@cea.fr

Henning Helmers
Fraunhofer Institute for Solar Energy Systems ISE
Freiburg, Germany
henning.helmers@ise.fraunhofer.de

***Abstract*—In micro-concentrating photovoltaics (micro-CPV), tiny solar cells (<1 mm²) are assembled on a circuit board on glass. To mount thousands of dies per square meter, a high throughput process is required which still yields alignment accuracy in the order of 10 µm. We developed a micro-CPV module technology where micro cells are accurately mounted directly on a circuit board on glass using a high throughput pick and place process combined with self-alignment based on the restoring force due to surface-tension of the liquid solder. In this work, we study how the self-alignment accuracy is influenced by the pad layout, solder volume and initial position of the die. We show that self-alignment significantly benefits from an induced motion, whether induced by initial displacement of the die or by flowing of molten solder along tracks. Furthermore, we found that lower solder volumes lead to higher alignment accuracies for dies on rectangular pads, whereas the dependence on solder volume is lower for pads with connected tracks where the solder flows out. Overall, alignment accuracies below 15 µm are demonstrated despite initial displacements up to 150 µm. Thus, self-alignment using surface tension of the liquid solder is suitable for micro-CPV.**

Keywords—Micro-concentrating photovoltaics (CPV), solar cell assembly, soldering, self-alignment, restoring force

I. INTRODUCTION

Concentrating photovoltaics (CPV) enable higher solar conversion efficiencies than conventional flat-plate solar panels due to the application of high-efficiency multijunction solar cells and improved efficiency under concentration [1]. At the same time, the amount of energy-intensive semiconductor material is reduced by the concentration factor of the concentrating optics used. In this process, the direct sun light is collected with lenses and focused on the solar cells. One major trend in CPV is the miniaturization of all components (micro-CPV), with typical solar cell dimensions well below 1 mm² [2, 3].

Fig. 1 (a) shows our micro-CPV module concept developed at Fraunhofer ISE [4, 5]. Sun light is concentrated on the solar cell by a factor of 1000 using a silicone-on-glass lens. Each cell is equipped with a spherical lens as secondary optical element. The solar cells are mounted directly on a circuit board on glass (chip-on-board approach). Given the small size of the components and the high concentration ratio, even small displacements can cause significant optical losses as the focused light misses the active cell area. Hence, precise alignment is crucial. In this work, we investigate the alignment accuracy of the solar cells on the circuit board on glass experimentally.

The circuit board serves for electrical interconnection and heat dissipation. The full area rear side contact of the cells is connected directly, and the front side contact is wire bonded to the circuit. The edges of the pad cannot be covered with solder resist. Misalignment of components or tracking uncertainties shift the focus point away from the cells center. Often a solder stop mask is used to define the die position. In this case, however, misalignment could burn conventional solder resist, which thus should be avoided. As shown in Fig. 1 (b) and (c) the direct focus on a glass plate with solder resist already yields to a visible burn spot after 30 minutes of sunlight. Due to the avoidance of a structured solder resist the accurate geometry of the receiving pads themselves must be used to define the solar cell position. For electrical interconnection of the rear side, the pads have partly connected tracks and partly gaps to isolate the front side from the rear. Further design considerations and a description of the manufacturing processes of the module concept are discussed in [4, 5].

In many sectors like flip-chip bonding, the standard for chip assembly is a pick and place process. Manufacturers of high throughput machines claim impressive assembly rates of more than 100'000 dies per hour with accuracies between 22 and 40 µm [6, 7]. The affection of the pick-and-place accuracy is determined with Raytrace3D, a raytracing tool developed at Fraunhofer ISE [8]. A displacement of the solar cells of 40 µm lead to an optical loss of 0.6%$_{abs}$. Thereby, for the solar cell displacement an optical loss of 0.1%$_{abs}$ is acceptable, which means an accuracy of ±16.6 µm [4].

For precise alignment, thus, we apply a combination of standard pick and place with surface tension driven self-alignment. First, solder paste is deposited on the receiving pads. Then, the solar cells are placed with low precision on the receiving pads (see Fig. 2, a). Next, during reflow, the solder paste melts and wets the surface of the pad and the rear side of the cell (see Fig. 2, b). The liquid solder develops a meniscus whose force induced by the surface tension, pulls the cell to the pad (see Fig. 2, c).

This work was funded by the German Federal Ministry for Economic Affairs and Climate Action (BMWK) under the "micro-CPV" project (#03EE1046A) and by the Institut Carnot Energies du Futur in the framework of the PVµCo project.

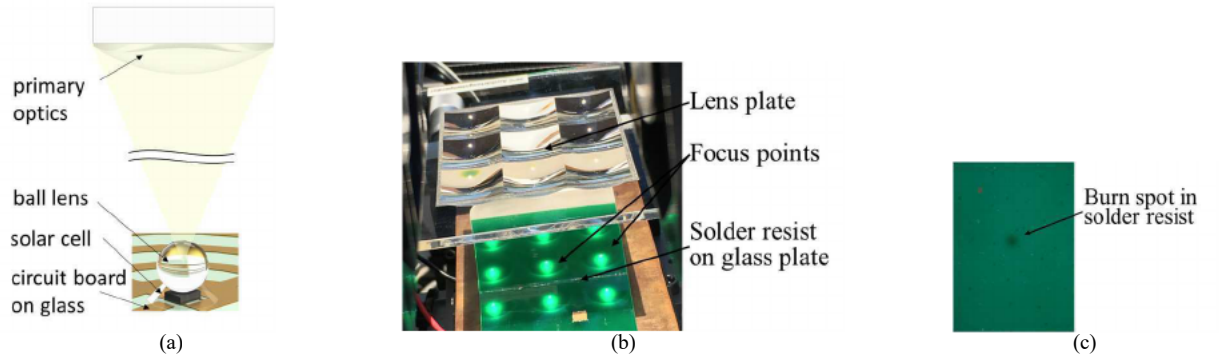

(a) (b) (c)

Fig. 1. (a) Sketch of a cell-lens unit of the micro-CPV module, developed at Fraunhofer ISE. The sun is focused with a silicone-on-glass primary lens onto a micro solar cell. The cell is assembled on a circuit board on glass and equipped with a secondary spherical lens. (b) Outdoor test: A 3x3 lens array focuses the light onto a glass plate which is covered with a green solder resist. (c) Microscope picture of the base plate after 30 min sun exposure. The burn spot is visible in the solder resist.

The self-alignment process is influenced by the solder volume, surface tension and viscosity, the wetting properties of the pad and the cell surface, the shape of die and pad and the initial displacement [9–12]. This work focuses on the influence of solder volume, pad layout and initial displacement. Note that a more detailed study is in preparation [13].

A force-based model can be used to analytically describe the self-alignment of a die [9, 12]. Fig. 3 shows a simplified sketch of the investigated case with a die (*S*) on a liquid depot (*L*) with straight flanks. The contact area between the liquid solder and the die is the rear side of the die. For self-alignment, the lateral forces are relevant, namely the force induced by the surface tension of the liquid solder F_{st} and the dynamic friction force F_v. The surface tension force acts on the boundary areas between the gaseous- liquid- solid (*G-L-S*) phases and depends on their surface tensions γ_i. It can be described by Eq. (1). The die and the pad have the same shape with the length l and the width w. The die is displaced by x from the pad and has the solder height h. The solder flank between the die and the pad has the angle α and it is assumed that the surfaces are completely wetted. Therefore, gradients of the surface tension between the liquid-solid phase are neglectable and the surface tension force can be described by Eq. (2) [9]

$$\vec{F}_{st} = \sum_{i}^{LS,LG,SG} \int \gamma_i \, d\vec{l} \tag{1}$$

$$\vec{F}_{st,x} \approx 2\gamma_{LG} w \cos(\alpha) \approx 2\gamma_{LG} w \frac{x}{\sqrt{x^2 + h^2}} \tag{2}$$

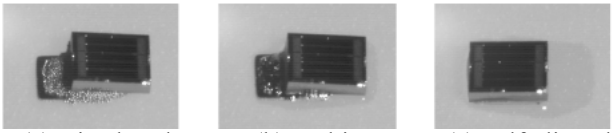

(a) Die placed inaccurately on solder paste (b) Melting process: Liquid solder wets pad and die surface (c) Self-aligned die to pad

Fig. 2. Mechanism of self-alignment using surface-tension of the liquid solder. Pictures of a high-speed camera of a micro solar cell (chip size 885x685 µm²) placed on a solder depot on a freestanding rectangular pad. Solder was melted by a heating plate.

The dynamic friction force between the liquid and the solid phases acts against self-alignment. The friction mainly originates from the viscosity η_L of the liquid solder. Simplified, the velocity v of the liquid solder is set equal to the die velocity and the area corresponds to the die rear side surface A_{LS} (3) [12].

$$\vec{F}_{v,x} \approx \eta_L A_{LS} \frac{v}{h} \tag{3}$$

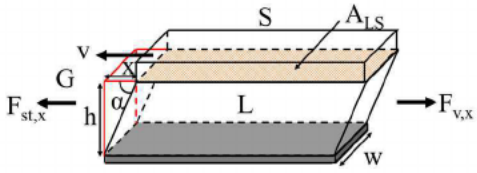

Fig. 3. Simplified sketch, sizes not to scale. A die (S) is displaced by the distance x on a liquid depot (L) with the height h. The contact area of die rear side and the solder is named A_{LS} and the angle between the gaseous (G) and liquid (L) phase is α. The die moves with the velocity v.

II. MATERIALS AND METHODS

Micro solar cell dies with an edge length of 885x685 µm² and a height of approximately 190 µm are placed on four different solder volumes and on two different pad layouts.

The pads are manufactured with a subtractive printed circuit board (PCB) process on a 3 mm glass substrate and consist of 30 µm copper and a chemical nickel/ gold finish. Fig. 4 (b) and (c) show pictures of the samples. One is a rectangular pad with an edge length by 27 µm smaller than the cell, named in the following *R-27*. The other pad is also rectangular but has additional connected tracks. Here, the edge length is smaller by 15 µm, named *I-15*. Before soldering, the pads are pre-treated with acetone and then ethanol.

Dies were mounted using stencil printing and die assembly at CEA LETI. SnAg3.0Cu0.5 solder paste with a flux content of 11.5±1.0% and particle size between 20 and 45 µm is applied. The stencil has a thickness of 200 µm and four different sizes for the openings between 615x454 µm² and 765x565 µm² (see TABLE I). The dies are assembled with a pick and place machine with an accuracy <5 µm. The dies are initially placed either in center position or intentionally displaced by 50 µm, 100 µm and 150 µm. Afterwards the solder is melted in a reflow oven, where the samples are kept 2.5 min above liquidus temperature of 217 °C. The resulting solder layer thickness for the

rectangular pad R_{-27} is between 28.1 and 50.9 µm and for layout I_{-15} between 5.3 and 15.4 µm. Based on the solder layer thickness on the pad R_{-27} the solder volumes were calculated and are between 16.0 and 28.9 nl. Note that these volumes are calculated from the solid state after soldering, and the liquid solder volumes are larger. For statistics, 20 samples are produced for each solder volume and initial displacement variation.

The alignment accuracy of the dies to the pads is measured with a coordinate measurement device that has an accuracy below 2 µm. First, the size and x-y-positions of the pads with respect to fiducials are measured. After soldering, the size and x-y-positions of the dies are determined in the same manner. From this data the offset is determined as the difference between cell center and pad center.

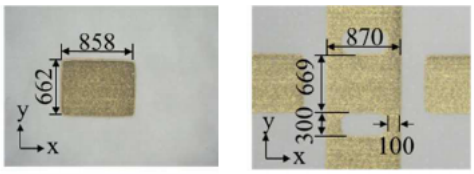

(a) Rectangular pad R_{-27} (b) Interconnected rectangular pad I_{-15}

Fig. 4. Microscope pictures of the different pad layouts. All sizes in µm.

TABLE I. STENCIL DESIGN

	Opening			
	A	***B***	***C***	***D***
Opening size [µm]	615x454	665x491	715x528	765x565
Measured solder thickness R_{-27} [µm]	28.1±3.2	35.3±4.5	40.1±2.6	50.9±5.4
Measured solder thickness I_{-15} [µm]	5.3±3.2	7.1±4.8	8.0±5.0	15.4±4.3
Volume based on measured solder thickness R_{-27} [nl]	16.0	20.1	22.8	28.9

III. RESULTS

The purpose of this study is to determine the influence of the pad layout, different solder volumes and initial displacements on the self-alignment accuracy of dies.

First, dies are initially displaced with four different solder volumes on the rectangular pad R_{-27}. Fig. 5 (a) shows the resulting offsets as a function of the initial displacement. The boxes represent the 25-75 percentiles, and the lines represent the entire observed range from minimum to maximum. Self-alignment is considered to be successful, when the cell is fully placed above the slightly smaller pad. Note that this includes left edge alignment, center alignment, and right edge alignment. Dashed lines mark this range, spun across $\pm\Delta l_R/2$. For pad R_{27} , $\pm\Delta l_R/2$ is ±13.5 µm. As a first observation, for the lowest solder volume of 16.0 nl (top), most of the dies are within this range. The median offset is close to the zero line up to an initial displacement of 100 µm. With an initial displacement of 150 µm, the median offset jumps to the edge of the self-alignment range $\pm\Delta l_R/2$ and scattering is reduced.

In Fig. 5 (a), from the top to the bottom graph, the solder volume is increased from 16.0 to 28.9 nl, i.e. the solder layer thicknesses are increased from 28.1 µm to 50.9 µm. For the medium solder volumes (blue and red data) a similar behavior as for the lowest solder volume is observed. In contrast, for the largest solder volume, the median offset shows no clear trend and with increasing solder volume, also the scattering increases. Increasing the solder thickness from 28.1 to 50.9 µm results in a relative increased scattering of 59% for ideal initial placement and of 60% for an initial displacement of 150 µm. Overall, for all solder volumes we observe decreased scattering with increased initial displacement. For a solder thickness of 28.1 µm the scattering reduces from ideal initial placement to 150 µm initial displacement by 46%, for 35.3 µm by 41%, for 40.1 µm by 38% and for 51 µm by 46%. Note that for all solder volumes, the highest measured offset is below 35 µm despite initial displacements up to 150 µm.

Fig. 5 (b) shows the behavior of dies on rectangular pads with connected tracks I_{-15}, again as a function of initial displacements up to 150 µm with increasing solder volume from top to bottom. Fig. 5 (c) shows a microscope picture of the interconnected after solder melting. As can be seen in the micrograph, after melting the solder leaves the pad and flows a certain distance along the connected tracks. Hence, a significant fraction of the solder is not underneath the chip anymore and the solder layer thickness is reduced to 5.3 to 15.4 µm. For pad I_{-15}, the self-alignment range $\pm\Delta l_I/2$ is given by ±7.5 µm. Most of the data and all medians are within this range. With the exception of ideal initial placement, all offsets are below 15 µm. In detail, 56% of the offsets are within ±5 µm and 87% within ±10 µm.

A comparison between the rectangular pad R_{-27} (Fig. 5, a) and the pad with connected tracks I_{-15} (Fig. 5, b) shows, that the scattering is reduced over all variations with pad I_{-15}. For example, for a solder volume of 20.1 nl, the scattering for ideal initial placement is reduced by 52% and for 150 µm initial displacement by 36%.

Besides the lateral offsets, out-of-plane rotations are visible dependent on the solder volumes, as sketched in the top of Fig. 5 (d). For the rectangular pad R_{-27} out-of-plane rotations in the horizontal axis were measured up to 2.6° for the lowest solder volume and up to 6.4° for the largest volume. The bottom of Fig. 5 (d) shows an x-ray image of a die placed on pad R_{-27}. The out-of-plane rotation can be recognized by the change in contrast from gray to black due to increasing solder thickness. In contrast, for the pads I_{-15} with connected tracks, no out-of-plane rotation was observed for the lowest solder volume. For the largest volume maximal outliers were 2.6°.

IV. DISCUSSION

Our study showed that for dies placed on rectangular pads R_{-27}, the cell to pad offsets are below 35 µm despite initial displacements up to 150 µm. A comparison of different solder volumes with equal initial displacement showed, that the scattering of the offsets increases with increased solder volume.

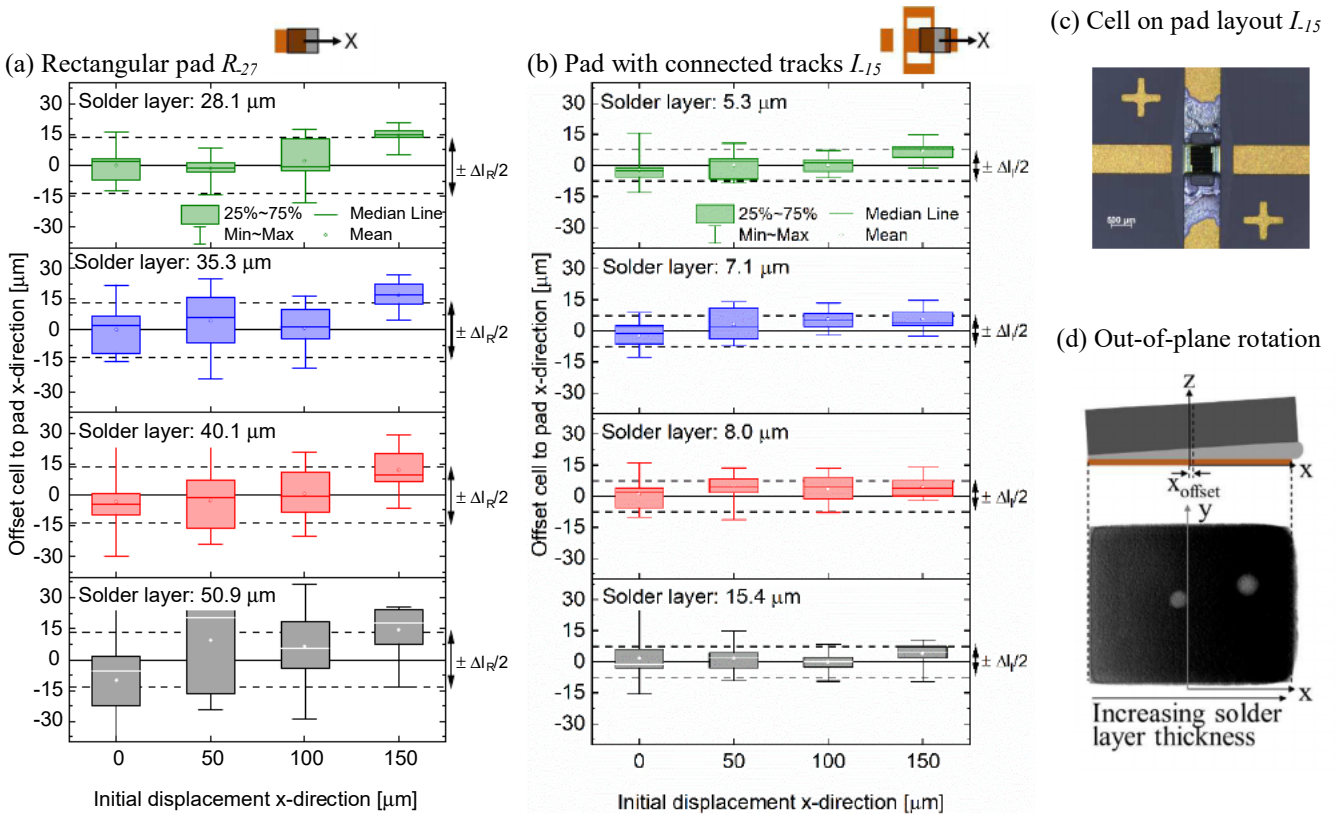

Fig. 5. (a), (b) Offset of the cell to pad dependent on the initial displacement in x-direction. From top to bottom: Solder volume is increased. The dashed line indicates the range of plus/minus half of cell to pad length difference. (a) For the rectangular pad R_{-27} the solder thickness is between 28.1 µm (top) and 50.9 µm (bottom). (b) For the rectangular pad I_{-15} the solder thickness is between 5.3 µm (top) and 15.4 µm (bottom). (c) Microscope image of a cell assembled on pad layout I_{-15} after the melting process. (d) X-ray image of a die mounted on a rectangular pad R_{-27}. Die is aligned on the left edge of the pad and is out-of-plane rotated in the horizontal axis. Above, an exaggerated sketch (side view) visualizes the out-of-plane rotation.

First, we conclude, that self-alignment using surface-tension of molten solder in principle works for all dies on rectangular pads with solder volumes between 16.0 and 28.9 nl. Yet, the observed scattering differs notably with the solder volume. This dependency can be explained by the restoring force. According to Eq. (2), the restoring force generally decreases with higher solder layer thickness h ($\sim x/\sqrt{x^2+h^2}$). Thus, the restoring force is influenced stronger by the thickness at small displacements ($x<<h$ → $\sim x/h$) than at larger displacements ($x>>h$ → $\sim 1/x$). For the investigated cases, the solder thickness h in the range of 28 to 56 µm and the initial displacements x up to 150 µm differ by only half an order of magnitude at maximum. Still, the relation between restoring force and solder volume is valid and explains, why the scattering increases with increased solder volume and especially for small offsets. However, the dynamic friction force, which acts again the restoring force, decreases with a thicker solder layer ($\sim \Delta v/h$) (3). Note, that the dynamic friction force is several orders of magnitude lower and thus, the surface tension force is dominant.

For all solder volumes, the median offsets are close to zero for low initial displacements, i.e. die center is to pad center alignment, whereas for larger initial displacement the median shifts towards the edge of the self-alignment range, which means edge-alignment. In general, the motion of the dies stops, when the restoring force vanishes or becomes overruled by the friction force. For the investigated samples it differs dependent on the initial displacement. Higher initial displacements tend to align on the edges and lower initial displacements to align center-to-center.

Furthermore, our study demonstrates for dies placed on pads I_{-15} with connected tracks, that all die to pad offsets are below 15 µm despite initial displacements up to 150 µm. Thus, the layout with connected tracks apparently improved the self-alignment.

It is important to emphasize that for pad I_{-15} we observe no clear dependence on initial displacement nor solder volume. Here, independent of the initial displacement, the liquid solder flows underneath the dies along the tracks. As a result of that, the solid solder thicknesses after assembly are reduced from 28-51 µm to 5-15 µm. The previously observed increased scattering with increasing solder volume vanishes. Overall, we conclude that induced motion, whether induced by initial misalignment or by flowing of the molten solder underneath the chip, is beneficial for the self-alignment process.

Finally, our observation of larger out-of-plane rotations for the rectangular pad layout R_{-27} compared with the layout I_{-15} with connected tracks is in line with the findings of Berthier et al. [14]. There, rectangular chips were soldered onto rectangular pads of the same size. During self-alignment, the out-of-plane rotation was not restored. An adjustment of the pads with additional bands decreased the out-of-plane rotation. However, in our case an additional effect has to be considered, which is the thinner solder layer for I_{-15} than for R_{-27}. Hence, lower out-of-plane rotations are possible.

V. Conclusion

Self-alignment of a die using surface tension of the molten solder was experimentally investigated regarding two pad layouts, four solder volumes, and initial displacements up to 150 µm. We find initial displacement of dies on rectangular pads to be beneficial for the self-alignment accuracy. The motion of the die due to surface tension induced restoring force supports overcoming opposing friction force and benefits the alignment accuracy. Furthermore, a lower solder volume is observed to be beneficial and reduces the scattering by approximately 60%. For pads with connected tracks, flowing solder positively affects the self-alignment, by helping to overcome static friction. For all investigated variations of solder volume and initial displacements, alignment accuracies below 15 µm were reached, 56% below 5 µm and 87% below 10 µm. It is remarked that the solder flow also reduces the resulting solder layer thickness to below 15.4 µm. Such thin solder layers can suffer from thermal cycling loads and long-term stability needs to be investigated in the future. Finally, ray tracing analysis of our micro-CPV module suggests that an alignment accuracy of 15 µm results in optical losses of less than $0.1\%_{abs}$.

Acknowledgment

The authors sincerely thank Philippe Voarino and Romain Cariou for hosting Elisa Kaiser at CEA INES and for enabling the die assembly at CEA LETI. We thank Alexander Dilger at Fraunhofer ISE for pick-and-place support, and all colleagues of the "III-V Photovoltaics and Concentrator Technology" department for continuous support. We thank EVYTRA GmbH (formerly FELA GmbH) for providing circuit boards on glass, and AZUR SPACE Solar Power GmbH for providing micro solar cells. The authors are responsible for the content of this work.

References

[1] M. Wiesenfarth, I. Anton, and A. W. Bett, "Challenges in the design of concentrator photovoltaic (CPV) modules to achieve highest efficiencies," *Applied Physics Reviews*, vol. 5, no. 4, p. 41601, 2018.

[2] C. Domínguez, N. Jost, S. Askins, M. Victoria, and I. Antón, "A review of the promises and challenges of micro-concentrator photovoltaics," in Ottawa, Canada, 2017, p. 80003.

[3] S. Paap, V. Gupta, A. Tauke-Pedretti, P. Resnick, C. Sanchez, G. Nielson, J. L. Cruz-Campa, B. Jared, J. Nelson, M. Okandan, and W. Sweatt, "Cost analysis of flat-plate concentrators employing microscale photovoltaic cells for high energy per unit area applications," in *2014 IEEE 40th Photovoltaic Specialist Conference (PVSC)*, 2014, pp. 2926–2929.

[4] E. Kaiser, P. Schöttl, M. Wiesenfarth, P. Nitz, and H. Helmers, "Effects of Manufacturing Tolerances on Micro-CPV Module Performance," in *18TH INTERNATIONAL CONFERENCE ON CONCENTRATOR PHOTOVOLTAIC SYSTEMS (CPV-18), to be published.*

[5] M. Wiesenfarth, D. Iankov, J. F. Martínez, P. Nitz, M. Steiner, F. Dimroth, and H. Helmers, "Technical boundaries of micro-CPV module components: How small is enough?," in *17TH INTERNATIONAL CONFERENCE ON CONCENTRATOR PHOTOVOLTAIC SYSTEMS (CPV-17)*, Freiburg, Germany / Online, 2022, p. 30008.

[6] JUKI Smart Solutions, "RX-8," [Online] Available: https://www.juki-smt.com/produkte/placement/placement-rx-8/. Accessed on: May 28 2023.

[7] ASMPT GmbH & Co. KG, "SPILACE X S: Maximale Kapazität für die Integrated Smart Factory," Feb. 2023. [Online] Available: https://smt.asmpt.com/de/produkte/placement-solutions/placement-heads/siplace-speedstar/. Accessed on: May 28 2023.

[8] P. Schöttl, G. Bern, P. Nitz, F. Torres, and L. Graf, "Raytrace3D by Fraunhofer ISE: Accurate and efficient ray tracing for concentrator optics," Fraunhofer Institut für Solare Energiesysteme ISE, 2022. [Online] Available: https://www.ise.fraunhofer.de/content/dam/ise/de/downloads/pdf/raytrace3d.pdf. Accessed on: May 20 2022.

[9] M. Mastrangeli, Q. Zhou, V. Sariola, and P. Lambert, "Surface tension-driven self-alignment," (eng), *Soft matter*, vol. 13, no. 2, pp. 304–327, 2017.

[10] H.-P. Park, G. Seo, S. Kim, and Y.-H. Kim, "Effects of Solder Volume and Reflow Conditions on Self-Alignment Accuracy for Fan-Out Package Applications," (En;en), *JEM*, vol. 47, no. 1, pp. 133–141, https://link.springer.com/article/10.1007/s11664-017-5883-0, 2018.

[11] S. Härter, "Qualifizierung des Montageprozesses hochminiaturisierter elektronischer Bauelemente," FAU University Press, 2020.

[12] O. Krammer and Z. Illyefalvi-Vitéz, "Investigating the self-alignment of chip components during reflow soldering," *Per. Pol. Elec. Eng.*, vol. 52, no. 1-2, p. 67, 2008.

[13] E. Kaiser, M. Wiesenfarth, V. Vareilles, M. Schneider-Ramelow, S. W. Glunz and H. Helmers, "Forced Motion Activated Self-Alignment of Micro-CPV Solar Cells," *IEEE J. Photovoltaics*, to be published.

[14] J. Berthier, K. A. Brakke, S. Mermoz, C. Frétigny, and L. Di Cioccio, "Stabilization of the tilt motion during capillary self-alignment of rectangular chips," *Sens. Actuators, A Phys.*, vol. 234, pp. 180–187, 2015.